Dynamic changes in anaerobic digester metabolic pathways and microbial populations during acclimatisation to increasing ammonium concentrations

Wei Zhang[1], Anna Alessi[2,3], Sonia Heaven[1*], James P.J. Chong[2], Charles J. Banks[1]

[1] Faculty of Engineering and Physical Sciences, University of Southampton, Southampton, SO17 1BJ, UK

[2] Department of Biology, University of York, Wentworth Way, York YO10 5DD, UK.

[3] Biorenewables Development Centre Ltd., 1 Hassacarr Close, Chessingham Park, Dunnington, York YO19 5SN, UK

* Correspondence: S.Heaven@soton.ac.uk

Abstract

Transitions in microbial community structure in response to increasing ammonia concentrations were determined by monitoring mesophilic anaerobic digesters seeded with a predominantly acetoclastic methanogenic community from a sewage sludge digester. Ammonia concentration was raised by switching the feed to source segregated domestic food waste and applying two organic loading rates (OLR) and hydraulic retention times (HRT) in paired digesters. One of each pair was dosed with trace elements (TE) known to be essential to the transition, with the other unsupplemented digester acting as a control. Samples taken during the trial were used to determine the metabolic pathway to methanogenesis using ^{14}C labelled acetate. Partitioning of ^{14}C between the product gases was interpreted via an equation to indicate the proportion produced by acetoclastic and hydrogenotrophic routes. Archaeal and selected bacterial groups were identified by 16S rRNA sequencing, to determine relative abundance and diversity. Acclimatisation for digesters with TE was relatively smooth, but OLR

and HRT influenced both metabolic route and community structure. The ^{14}C ratio could be used quantitatively and, when interpreted alongside archaeal community structure, showed that at longer HRT and lower loading *Methanobacteriaceae* were dominant and hydrogenotrophic activity accounted for 77% of methane production. At the higher OLR and shorter HRT, *Methanosarcinaceae* were dominant with the ^{14}C ratio indicating simultaneous production of methane by acetoclastic and hydrogenotrophic pathways: the first reported observation of this in digestion under mesophilic conditions. Digesters without TE supplementation showed similar initial changes but, as expected failed to complete the transition to stable operation.

Keywords anaerobic digestion, hydrogenotrophic methanogenesis, acetoclastic methanogenesis, ^{14}C labelling, ammonia, trace elements

Abbreviations

ASV, Amplicon Sequence Variant Table; COD, Chemical Oxygen Demand; CSTR, Continuously-Stirred Tank Reactor; FAN, Free Ammonia Nitrogen; HRT, Hydraulic Retention Time; IA, Intermediate Alkalinity; OLR, Organic Loading Rate; OTU, Operational Taxonomic Unit; PA, Partial Alkalinity; SAOB, Syntrophic Acetate Oxidising Bacteria; SMP, Specific Methane Production; TAN, Total Ammonia Nitrogen; TE, Trace Element; TKN, Total Kjeldahl Nitrogen; TA, Total Alkalinity; TS, Total Solids; VBP, Volumetric Biogas Production; VFA, Volatile Fatty Acid; VS, Volatile Solids; WW, Wet Weight

1 Introduction

In digestion of low nitrogen feedstocks two pathways to methane production are utilised, with approximately 60-70% of CH_4 produced by direct cleavage of acetate via acetoclastic methanogenesis, and the remaining 30-40% mainly formed from H_2 and CO_2 by hydrogenotrophic methanogens (Jerris and McCarty, 1965). In a typical digester fed on municipal wastewater biosolids, the dominant methane producers are the acetoclastic *Methanosaetaceae* (Karakashev et al., 2005). When a high nitrogen feedstock is introduced to such an inoculum, *Methanosaetaceae* and other methanogens with low tolerance for ammonia may suffer inhibition. This inhibitory effect was first noted in the 1960s (McCarty, 1964), and has since been widely discussed, with several recent reviews of the topic (Rajagopal et al., 2013; Yenigun and Demirel, 2013; Jiang et al., 2019). By the late 1970s it was realised that digesters could become adapted to high ammonia concentrations (e.g. Van Velsen, 1979), and the first practical steps towards digestion of ammonia-rich feedstocks were suggested in the work of Angelidaki and Ahring (1993). The mechanism of inhibition was initially unclear, but by the mid-1980s some research had indicated hydrogenotrophic methanogens were more tolerant than acetoclastic (Koster and Lettinga, 1984). It is now considered that at high ammonia concentrations stable methanogenesis can be achieved if there is a change in the methanogenic community and pathway from acetoclastic to hydrogenotrophic methanogenesis, with syntrophic acetate oxidation occurring as an essential step (Schnürer et al., 1999). Schnürer and Nordberg (2008) applied a ^{14}C labelling technique to demonstrate this shift in pathway. This change, and its reversibility after ammonia stripping, was subsequently verified for food waste digestion (Jiang et al., 2018; Serna et al., 2014), and is further supported by the observations of Karakashev et al. (2006) and others on full-scale commercial digesters, which also indicate the importance of syntrophic acetate oxidation in establishing stable methanogenic communities of this type.

The above transition is only possible if each of the reactions can be catalysed, and the essential role of selenium in allowing acclimatisation to increasing ammonia concentrations in food waste digestion was first noted by Banks et al. (2012). This element alleviates the slow progressive accumulation of propionic acid which was characteristic both of food waste digesters (Banks et al., 2008), and of other digesters operating at high ammonia concentrations (Resch et al., 2011; Molaey et al., 2018). Selenium appears to be essential in promoting the conversion of propionic acid, which has an uneven carbon chain length, into H_2 and CO_2 via formate, and in forming the seleno-cysteine complex necessary for formate dehydrogenase production (Jones and Stadtman, 1981; Wood et al., 2003). The typical volatile fatty acid (VFA) 'signature' observed in food waste digesters in response to increasing ammonia concentrations shows an initial acetic acid peak that is consumed in advance of the build-up of propionate and other longer chain VFA. This initial peak has been interpreted as resulting from the loss of acetoclastic activity: its subsequent decline is a result of the establishment of syntrophic acetate oxidation, but the accumulation of propionate suggests that syntrophic oxidation of longer chain VFA is at least partially inhibited. Eventually the buffering capacity of the digester is overcome by the acid accumulation, leading to a fall in pH and inhibition of all methanogenic activity. When the trace element requirements for both acetate and propionate oxidation are satisfied, the stable digestion of food waste at ammonia concentrations, which were once thought to be inhibitory under mesophilic conditions, can be achieved. Under thermophilic conditions this strategy of trace element addition is not effective (Yirong et al., 2015, 2017), and in this case stable operation can only be achieved by maintaining the free ammonia concentration below a critical threshold e.g. by ammonia stripping or dilution (Zhang et al., 2017a and b).

99 The commercial significance of understanding the process of acclimatisation to ammonia and
100 some of the factors that regulate it has been high. It has allowed digester operators the option
101 of using food waste from domestic and commercial sources as a high potential energy substrate
102 without dilution. This was not always so, as the material has an intrinsically high protein
103 content which on hydrolysis releases ammonia at concentrations previously considered
104 inhibitory, with total ammonia nitrogen (TAN) typically in excess of 5 g N L^{-1} promoting
105 changes in both the pH and alkalinity of the system (Banks et al., 2011; Zhang et al., 2012). As
106 a consequence of overcoming this limitation, anaerobic digestion of food waste is now
107 recognised in the food waste hierarchy as the best route to recovering value after all other
108 options for reduction and reuse have been considered; and is now used in many parts of the
109 world for both energy production and nutrient recycling from food wastes (Banks et al., 2018).
110
111 Better understanding of factors affecting the transition to and dominance of hydrogenotrophic
112 methanogenesis is also of value for other feedstocks and applications: for example to assist in
113 the establishment and maintenance of stable mixed culture communities for biomethanisation
114 of CO_2. This topic has recently attracted considerable attention, as it offers a means of
115 converting surplus renewable electricity into a storable and infrastructure-compatible fuel via
116 electrolytic hydrogen production (Aryal et al., 2018). While many approaches focus on high-
117 rate and pure culture systems, in situ mixed culture conversion is also of interest as a means of
118 increasing methane yield and upgrading biogas methane content from conventional feedstocks
119 (Luo et al., 2013a and b). Recent work showing the feasibility of upgrading biogas from
120 multiple digesters in one (Tao et al., 2019) supports this potential for application in large-scale
121 conventional digestion of food wastes and sludges, making more efficient use of existing
122 capacity.
123

While it is now widely recognised that acclimatisation of anaerobic digesters to ammonia can occur, previous studies using ^{14}C labelling to identify the associated change in methanogenic pathway have mainly reported results for full-scale commercial digesters at high and low ammonia concentrations (Schnürer et al., 1999; Karakashev et al., 2005; Fotidis et al. 2014). Only a few have attempted to observe the transition (Schnürer and Nordberg, 2008) or to compare known points in the process (Serna et al., 2014; Sun et al., 2016; Jiang et al., 2018); and none have linked the dynamic changes in pathway to changes in methanogenic population over the transition period. The ^{14}C labelling technique used to demonstrate the shift in metabolic pathway is based on the splitting of the C-C bond between the methyl and carboxyl group of acetic acid, with CH_4 being formed from the labelled methyl group while CO_2 is formed from the carboxyl group in acetoclastic methanogenesis (Ferry, 1993). A pure acetoclastic methanogenic community will thus channel all ^{14}C labelled acetate to $^{14}CH_4$, while a hydrogenotrophic methanogenic community forming biogas via syntrophic acetate oxidation will give an equal distribution of $^{14}CO_2$ and $^{14}CH_4$. In practice the results of ^{14}C labelling assays are rarely clear cut, and the ratio of the partition is often used simply as an indication of the dominant route (Fotidis et al., 2013). Jiang et al. (2018), however, derived an equation to quantify the proportion of carbon going by each route based on the ratio of attached ^{14}C labels.

The current study is the first to trial the application of this equation throughout the transition period in order to investigate its potential quantitative significance. It also presents one of the first detailed analyses of dynamic changes in the microbial population that occur during the shift from a predominantly acetoclastic population to a predominantly hydrogenotrophic pathway and population under increasing ammonia concentrations. These changes were mapped using chemical/biochemical analysis of the digestate, biofunctional information obtained from a ^{14}C labelling assay, and microbial identification analysis based on 16S rRNA

gene sequencing. Food waste was used as the substrate for the experiments as the acclimatisation process has been previously demonstrated (Banks et al., 2012): using Selenium as the 'key' to turn on the shift in pathway allowed a population transitioning to hydrogenotrophic metabolism through syntrophic acetate oxidation to be compared to one where this transition could not be achieved due to blockage of at least part of the metabolic pathway attributed to metallo-enzyme deficiencies.

2 Materials and methods

2.1 Inoculum and substrate

The inoculum was taken from a mesophilic anaerobic digester treating municipal wastewater biosolids in Millbrook, Southampton, UK.

Source separated food waste was collected from Otterbourne waste transfer station in Hampshire, UK. After collection, the material was manually sorted to remove a small proportion of oversized or unbiodegradable items such as plastic bags, garden rubbish and large bones or seeds. The material was homogenized using a S52/010 macerating grinder (Imperial Machine Company Ltd, UK), then mixed thoroughly, packed into 4-L plastic containers and frozen at -20 ^{o}C. Before use, the frozen food waste was thawed at ambient temperature then stored at 4 ^{o}C and used within a short period.

2.2 Digesters and semi-continuous digestion

173 Semi-continuous digestion was carried out in 4 no. 5-L continuously-stirred tank reactors
174 (CSTR). These were constructed in PVC with a top flange to which a top plate was secured by
175 stainless steel bolts, with a closed-pore neoprene gasket to provide a gas-tight seal. The top
176 plate was fitted with a gas outlet and a feed port sealed with a rubber bung. A DC motor
177 mounted on the top plate was coupled to an asymmetric bar stirrer through a draught tube with
178 a gas-tight compression seal. Digester contents were continuously stirred at 40 rpm, with
179 digestate removed from a 15 mm diameter outlet port at the base of the digester. Temperature
180 was maintained at 35 +/- 0.5 ºC by water circulating through an external heating coil. Gas
181 production was measured continuously by the alternate filling and discharging of a calibrated
182 cell, with each discharge logged via a labjack (labjack Ltd, UK) computer interface. Gas
183 counter calibration was checked twice per week using gas-impermeable bags connected to the
184 gas counter outlet, with gas volumes measured in a weight-type displacement gasometer
185 (Walker et al., 2009). All gas volumes are reported as dry gas at a standard temperature and
186 pressure of 0 ºC and 101.325 kPa.
187
188 The four digesters were fed over a period of 180 days on the source separated food waste. Two
189 digesters (M1 and M2) were fed at an organic loading rate (OLR) of 3 kg VS m^{-3} day^{-1}, and
190 the other two (M3 and M4) at 5 kg VS m^{-3} day^{-1}. Feed was added daily and digestate removed
191 once per week to maintain a working volume of 4 L. The digesters were monitored on a weekly
192 basis for pH, TAN, alkalinity, total and volatile solids and VFA concentrations.
193
194 M2 and M4 were supplemented once per week with a trace element (TE) solution to maintain
195 an additional working concentration in the digestate of the following elements (mg L^{-1}): Cobalt
196 1.0, Nickel 1.0, Molybdenum 0.2, Selenium 0.2, Tungsten 0.2, based on Banks et al. (2012).
197 No TE solution was added to M1 or M3.

198

199 2.3 Analytical methods

200

201 Total solids (TS) and volatile solids (VS) determination was carried out in accordance with
202 Standard Method 2540 G (APHA, 2005). pH was measured using a Jenway 3010 meter (Bibby
203 Scientific Ltd, UK) with a combination glass electrode, calibrated in buffers at pH 4, 7 and 9.2.
204 Alkalinity was measured by titration according to Standard Method 2320B (APHA, 2005).
205 TAN was determined according to Standard Method 4500-NH3 B and C (APHA, 2005). Total
206 Kjeldahl Nitrogen (TKN) was determined as TAN after acid digestion of the material. Soluble
207 Chemical Oxygen Demand (COD) was determined after filtration through a 0.45 μm syringe
208 filter (Merck Millipore, SLCR033NS) followed by centrifugation (Eppendorf 5417 C/R,
209 Eppendorf, Hamburg Germany) at 5000 rpm for 5 min, according to according to Environment
210 Agency (2007). Samples for VFA analysis were prepared by centrifugation at 13,000 *g* for 30
211 min, and the supernatant was acidified to 10% (v/v) with formic acid. VFA concentrations were
212 measured using a Shimazdu GC-2010 gas chromatograph (Shimadzu, UK) with a flame
213 ionization detector and a capillary column (SGE Europe Ltd, UK) and Helium as the carrier
214 gas. The GC was calibrated with a standard solution containing acetic, propionic, iso-butyric,
215 n-butyric, iso-valeric, valeric, hexanoic and heptanoic acids, at three dilutions to give
216 individual acid concentrations of 50, 250 and 500 mg L^{-1} respectively. Biogas composition was
217 quantified using a Varian Star 3400 CX gas chromatograph (Varian Ltd, UK). The GC was
218 fitted with a Hayesep C column and used argon as the carrier gas at a flow of 50 mL min^{-1} with
219 a thermal conductivity detector. The GC was calibrated with a standard gas containing 35%
220 CO_2 and 65% CH_4 v/v (BOC, UK).

221

222 2.4 Radio-isotope labelling experiments

A Carbon-14 tracer technique was used to determine the metabolic pathway for methane production. Each sample was mixed with anaerobic medium as described in Jiang et al. (2018) in the ratio of 1:2 v/v. 10 KBq of $^{14}CH_3COONa$ (MP biomedical, USA) was added into 45 mL of the sample/medium mixture and incubated in 119 mL crimp-top serum bottles at 37 °C for 48 hours. CO_2 and CH_4 produced in the headspace were separately collected in alkali traps containing 20 mL of 1 M NaOH solution: before collection, the CH_4 was oxidised to CO_2 in a tube furnace consisting of a heating block containing an embedded quartz tube (6.2 mm OD, 4 mm ID, 180 mm length, H. Baumbach & Co Ltd, UK) packed with copper (II) oxide. The furnace operating temperature was regulated at 800 ± 5 °C using a temperature controller (Omega DP7004, UK). After collection, 0.4 mL of NaOH solution from each alkali trap and 0.4 mL of the sample/medium mixture (after centrifugation) were added to 3.6 mL Gold Star multi-purpose liquid scintillation cocktail (Meridian 56 Biotechnologies Ltd, UK) and counted in a PerkinElmer 2450 MicroBeta^2 liquid scintillation counter (PerkinElmer Life and Analytical Sciences, USA).

The proportion of methane generated by acetoclastic and hydrogenotrophic routes was estimated according to Equation 1 based on Jiang et al. (2018)

$$P_a = 1/(^{14}CO_2/^{14}CH_4 + 1)$$ Equation (1)

Where P_a is the proportion of methane produced via acetoclastic methanogenesis and $^{14}CO_2$ and $^{14}CH_4$ are the volumes of labelled carbon dioxide and labelled methane, respectively, produced from acetate labelled on the methyl group.

2.5 16S rRNA sequencing

DNA extraction

The microbial pellet was separated from the supernatant by centrifugation at 8,000 x g for 10 minutes at 4 ^{o}C. The Power Soil DNA (MOBIO) extraction protocol was applied to 200 mg of pelleted biomass according to the manufacturer's recommendations.

PCR based analysis

Metagenomic DNA (50 ng) extracted from the digester samples (n = 53) was used directly to amplify 16S rRNA genes using primers containing Illumina adapters designed to cover the V4 region (S-D-Arch-0519-a-S-15 = CAGCMGCCGCGGTAA, S-D-Bact-0785-b-A-18 TACNVGGGTATCTAATCC). PCR reactions were carried out in 50 µL volumes containing 200 µM of dNTPs, 0.5 µM of each primer, 0.02 U Phusion High-Fidelity DNA Polymerase (Finnzymes OY, Finland) and 5x Phusion HF Buffer containing 1.5mM $MgCl_2$. The following PCR conditions were used: initial denaturation at 98 ^{o}C for 2 min, followed by 25 cycles consisting of denaturation (98 ^{o}C for 5 sec), annealing (52 ^{o}C for 30 sec) and extension (72 ^{o}C for 30 sec) and a final extension step at 72 ^{o}C for 5 min. The expected amplicon size for 16S rRNA product was approximately 280 bp. The amplified fragments were purified with Agencourt AMPure XP (Beckman Coulter, UK). The quantity of purified PCR products was analysed by Qubit fluorometer (Life Technologies, USA).

Illumina sequencing of 16S rRNA tags

Illumina libraries were prepared using a Nextera XT kit, following the company's recommendations for 16S PCR amplicon barcoding, clean up and libraries normalisation. All indexed libraries were quantified using a Qubit fluorometric system, diluted to 4 nM and mixed

in equal volumes of uniquely barcoded samples. Pooled libraries and PhiX control were denatured with freshly-made 0.2 N NaOH, diluted to 5 pM with hybridization buffer and mixed together in the ratio 3.3:1 v/v. Samples were heated at 96 ^{o}C for 2 min and cooled for 5 min then immediately loaded on a MiSeq v3 cartridge for 300 bp sequencing in both directions. The completed run was demultiplexed with Illumina's Casava software.

Data analysis

The Illumina-sequenced paired-end fastq files that had been split (or "demultiplexed") by sample and from which the adapters had been removed were used for the data analysis using the DADA2 (version 1.6.0) pipeline (Callahan et al., 2016). Non-biological nucleotides (primers) were trimmed from fastq raw data using the FastX-Toolkit (Hannonlab, Cold Spring Harbor Laboratory, NY, USA). The forward and reverse reads were filtered by truncating at 250 and 200 bp respectively with the default parameters at maxEE=2, truncQ=5, maxN=0. The error rate was determined using the DADA2 parametric error model (err). The pair-end reads were merged to obtain the full denoised sequence and dereplicated prior to building an amplicon sequence variant table (ASV). The sequence table is a matrix with rows corresponding to (and named by) the samples, and columns corresponding to (and named by) the sequence variants. Chimeric sequences were identified and removed from the final operational taxonomic unit (out) table. The taxonomy of each OTU was assigned using DADA2 package with a native implementation of the naive Bayesian classifier method. DADA2 formatted reference database Silva version 132 (Quast et al., 2012) was used for this purpose. Detailed R script to data analysis is provided in Supplementary Information section S1. Subsequent visualization and statistical analysis used Prism7 (GraphPad Software, San Diego, CA).

298 It should be noted that this technique does not distinguish between live and dead organisms,
299 and may also identify undegraded fragments of 16S rRNA from the latter. The significance of
300 this for the study of a transition period is briefly discussed in Supplementary Information S3.
301
302 **3 Results and discussion**
303
304 3.1 Feedstock and inoculum properties
305
306 The inoculum was taken from a mesophilic anaerobic digester receiving a feed of co-settled
307 primary and secondary sewage sludge at a municipal wastewater treatment plant. Its
308 characteristics were typical of material from this type of digester, with a pH around 7.5, TAN
309 1.5 g N kg^{-1} wet weight (WW), total VFA concentrations < 100 mg COD L^{-1}, and total
310 alkalinity (TA) around 7.5 g $CaCO_3$ kg^{-1} WW. The characteristics of the food waste are shown
311 in Table 1 and are also typical of this type of material (Banks et al., 2018). At the applied OLR
312 of 3 and 5 g VS L^{-1} day^{-1} the corresponding average hydraulic retention times (HRT) in the
313 digesters were respectively 69 and 41 days.
314
315 3.2 Digester operation and performance
316
317 Figure 1 shows changes in key digestion stability parameters over the duration of the
318 experiment. In M3, the more highly loaded of the two digesters not receiving trace elements,
319 there was a rapid accumulation of VFA from day 55 onwards (Figure 1a) reaching 9.6 g COD
320 L^{-1} by day 70. On day 72 feeding was suspended for 5 days, during which the VFA
321 concentration fell slightly. After feeding was re-started the total VFA concentration increased
322 again, and by day 83 had reached 18.2 g COD L^{-1}. At this point the pH dropped sharply to 7.3

(Figure 1b), the intermediate alkalinity (IA) increased, partial alkalinity (PA) fell and the IA/PA ratio rose to 1.05 (Figure 1c-e). A similar pattern was seen in M1, the lower-loaded digester without TE supplementation; but, as expected due to the longer HRT, the onset was delayed until around day 110. Total VFA concentrations in M1 increased from day 70 and plateaued at around 1.5 g COD L^{-1} (Figure 1a), before rising again from day 97 to reach 15.9 g COD L^{-1} on day 126, by which point the IA/PA had risen to 1.46 and the pH fell to 7.37.

In both cases the onset of VFA accumulation corresponded to the TAN concentration reaching around 3.6 g N kg^{-1} WW (Figure 1f), in good agreement with the results of a previous study using a similar food waste (Yirong et al. 2017). This behaviour has also been reported by other researchers: once a threshold TAN concentration is exceeded, inhibition of acetoclastic methanogenesis occurs, resulting in accumulation of first acetic acid and then longer-chain VFA, due to product-induced inhibition of acetogenesis (Karakashev et al., 2006; Schnürer and Nordberg, 2008). In M1 the VFA primarily consisted of acetic acid, although small amounts of longer chain VFA appeared after day 70 and the propionic acid concentration reached 0.7 g L^{-1} by day 126. In M3 propionic acid had reached 1.9 g L^{-1} by day 83.

In M2 and M4, the digesters with TE supplementation, total VFA concentrations also began to rise on days 70 and 55 respectively when TAN reached around 3.6 g N kg^{-1} WW; but then fell from their peak values of 4.5 and 8.5 g COD L^{-1} to < 0.5 g COD L^{-1} by days 90 and 126 in M2 and M4, respectively. This was despite the continuing increase in TAN, which reached final values of 5.3 and 5.4 g N kg^{-1} WW in M2 and M4, respectively. Because of the high TAN and the relatively low VFA concentrations, the pH in these digesters slowly increased from 7.6 to 8.0 over the experimental period. The IA/PA ratios remained relatively stable at around 0.4

347 throughout the trial period, apart from small increases during the transient VFA peaks (Figure
348 1e).
349
350 Digestate solids content and VS/TS ratios (Figure 1g) were similar in pairs of digesters at the
351 same OLR, with the slightly higher values in M3 and M4 probably reflecting an increase in
352 microbial biomass at the higher OLR of 5 g VS L^{-1} day^{-1}. Soluble COD content also showed
353 reasonable agreement for digesters at the same OLR (Figure 1h) until VFA accumulation
354 occurred in the unsupplemented digesters. VFA typically represented less than 20% of the
355 soluble COD, which averaged around 8 g L^{-1} higher in M4 than in M2 from day 77 onwards.
356 These results support previous observations on the relatively high concentration of soluble
357 microbial products and extracellular polymeric substances present in food waste digesters,
358 which are a cause of poor dewaterability (Lü et al., 2015).
359
360 The volumetric biogas production (VBP, in litres of biogas per litre of digester working volume
361 per day) and the specific methane production (SMP, in litres of CH_4 per g of feedstock VS
362 added) are shown in Figure 2. In the TE-supplemented digesters M2 and M4 these were
363 relatively consistent throughout the experimental period, apart from for short periods
364 corresponding to the temporary increase in VFA after the TAN concentration in each of these
365 digesters exceeded 3.6 g N kg^{-1} WW. The average SMP was around 0.45 L CH_4 g^{-1} VS , and
366 the VBP was between 2.0-2.5 L L^{-1} day^{-1} at the lower OLR (M2) and 3.5-4.0 L L^{-1} day^{-1} at the
367 higher OLR (M4). In digesters M1 and M3 without TE supplementation, both SMP and VBP
368 both showed a progressive decline after the threshold TAN concentration was reached, and
369 then a rapid fall once the buffering capacity of the system was overcome and the pH dropped
370 sharply. These digesters were considered to be at the point of final failure by days 127 and 83
371 corresponding to around 1.8 and 2.0 HRT respectively, and feeding was stopped at this point.

Digesters M2 and M4 were operated for 180 days, with samples for final analysis of most monitoring parameters taken on day 174. A period of 3 HRT is normally considered necessary to achieve steady -state operation, based on washout of around 95% of the digester's initial contents. M4 with a HRT of 41 days ran for 4.2 HRT in total but M2 only achieved 2.5 HRT, corresponding to approximately 98 and 92% displacement of the initial digester contents, respectively. The final values for M2 are thus not fully representative of steady-state conditions, although stabilisation of key values is evident in Figure 1 and 2. Since the focus of this study is specifically on the transition period, however, this was not considered to be a major issue.

The performance of all digesters thus demonstrated the patterns consistently observed on previous occasions for this type of feedstock (Banks et al., 2012; Zhang et al., 2017), with TE supplementation once again shown to be essential in enabling stable operation at the applied loadings and resulting TAN concentrations in each case.

3.3 Changes in microbial community and metabolic function in response to increasing TAN concentrations

3.3.1 Classification of microbial taxa

Amplicon sequencing of 16S rRNA genes from the digesters resulted in 9.68 million pair-end reads (n = 60, average = 182,577, standard error of mean [s.e.m] = 6,028) of which 5.56 million were retained after quality control trimming and removal of chimeric reads (see Supplementary Information Table S2). The initial OTU table contained 2,046 individual bacterial and archaeal OTUs. OTUs where the number of reads across all the samples was lower than 10 (so-called

singletons) were removed, resulting in 378 OTUs remaining for final analysis. The archaeal communities were exclusively classified to families within the Euryarchaeota, mainly *Methanosarcinaceae*, *Methanosaetaceae*, and *Methanobacteriaceae*. The evolution of these is discussed below. Changes in bacterial communities are briefly discussed in the Supplementary Information section S2.

3.3.2 Response to increasing TAN in lower loaded, TE-supplemented digester M2

Figure 3a shows archaeal community structure, TAN and acetic acid concentrations and ^{14}C ratios in digester M2. Until day 70 only a small number of Archaea were observed, and meaningful analysis of the relative abundance was not possible. By day 70 the TAN concentration was 3.6 g N kg^{-1} WW (FAN ~0.25 g N kg^{-1} WW) and acetoclastic *Methanosaetaceae* were the dominant family, making up 96.4% of the observed Archaea. The ^{14}C ratio was 0.25, indicating that methane production was mainly by the acetoclastic route. As noted earlier, from day 70 onwards there was a small increase in the acetic acid concentration, which remained steady at around 1 g L^{-1} until day 104. At this point the TAN concentration in M2 had reached 4.3 g N kg^{-1} WW (FAN ~0.41 g N kg^{-1} WW), and a sharp increase in acetic acid concentration was seen. *Methanosaetaceae* were still dominant in the archaeal community (92.5%), however, and the ^{14}C ratio was 0.15, confirming that acetoclastic methanogenesis was still the primary route to methane formation.

The acetic acid concentration continued to rise, reaching 3.7 g L^{-1} on day 118 and remaining around this value until day 126. This accumulation was accompanied by a gradual increase in TAN, which had reached 4.6 g N kg^{-1} WW by day 118. The relative abundance of *Methanosaetaceae* fell in this period and the proportion of hydrogenotrophic

Methanobacteriaceae began to increase, reaching 41% of the archaeal community by day 126. The ^{14}C ratio also rose to 0.72 by day 126, indicating that over half of methane production was now by the hydrogenotrophic route.

From day 140 onwards the *Methanobacteriaceae* were the dominant family, accompanied by a slight increase in the relative abundance (up to 2%) in the relative abundance of other Euryarchaeota, while the proportion of *Methanosaetaceae* fell. By day 160 the relative abundance of *Methanobacteriaceae* was 68% compared to 18-22% *Methanosaetaceae*, with a ^{14}C ratio of 3.53 indicating a strongly hydrogenotrophic pathway to methane production. Based on Equation 1, these results indicated that between days 118 and 146 hydrogenotrophic methane production had increased from 14% to 77% of the total.

It was also noted that on day 133 there was a small recovery in the relative abundance of *Methanosaetaceae*, corresponding to the sharp fall in acetic acid concentration, which then remained around 1 g L^{-1}.

3.3.3 Response to increasing TAN in higher loaded, TE-supplemented digester M4

Figure 3b shows the archaeal community structure, TAN and acetic acid concentrations and ^{14}C ratios in digester M4. By day 55 the TAN concentration had reached 3.6 g N kg^{-1} WW. Until this point the acetoclastic *Methanosaetaceae* were dominant, with a relative abundance of around 96% (Figure 3b), and the ^{14}C ratio of < 0.3 indicated predominantly acetoclastic methane formation. Between days 55 to 77 the relative abundance of *Methanosaetaceae* fell, while the *Methanobacteriaceae* increased from 6 to 42%. At this point, the trends in population appeared similar to the early stages of transition in M2 between days 104 and 126 (Figure 3a);

447 but with the difference that acetic acid concentrations remained low and no significant change
448 was observed in the ^{14}C ratio, which was still 0.14 on day 70.
449
450 From day 77 there was a very sharp increase in the acetic acid concentration, which reached 7
451 g L^{-1} by day 90. This was accompanied by an increase in TAN from 4.0 to 4.4 g N kg^{-1} WW,
452 passing through the value at which the acetic peak had appeared in M2. On days 83 and 90
453 there was a temporary recovery in *Methanosaetaceae* and a corresponding fall in the relative
454 abundance of *Methanobacteriaceae*. The acetic acid concentration remained high until day 97,
455 however, when a large increase in *Methanosarcinaceae* was observed, up to 54% of the
456 archaeal population. Between days 90-97 the ^{14}C ratio rose from 0.22 to 0.46, indicating that
457 the switch in pathway from dominantly acetoclastic towards hydrogenotrophic methanogenesis
458 had begun. This transition continued, with the relative abundance of *Methanosarcinaceae*
459 increasing from 8% on day 90 to 93% on day 160. The ^{14}C ratio also rose, peaking at 2.56 on
460 day 146 before falling slightly in the final two weeks of operation. The TAN concentration in
461 this final period was around 4.9 g N kg^{-1} WW (FAN ~0.5-0.8 g N kg^{-1} WW), and
462 *Methanosarcinaceae* continued to dominate the community, with *Methanobacteriaceae* at
463 around 6% and other Euryarchaeota accounting for around 1%.
464
465 3.3.4 Comparison of responses at different loading rates and HRT
466
467 The operating protocols adopted for M2 and M4 were the same except that the loading rate was
468 higher and the HRT consequently shorter in M4 than M2. Both digesters showed a transition
469 to predominantly hydrogenotrophic methanogenesis that was triggered at a threshold TAN
470 concentration of around 4.3 g N kg^{-1} WW; and both exhibited a characteristic increase in acetic
471 acid concentration, followed by a fall which could be attributed to the establishment of

472 syntrophic acetate oxidation. Both digesters also showed a period where there was a near-linear
473 increase in the ^{14}C ratio. In M2 this occurred between days 118-146, with a slope of 0.117 day^{-1}
474 ($R^2 = 0.9635$, n = 5, $p < 0.005$); while in M4 it occurred between days 90-146, with a slope
475 of 0.043 day^{-1} ($R^2 = 0.9960$, n = 9, $p < 5 \times 10^{-9}$). T-testing indicated that the two slopes were
476 significantly different ($p < 0.0005$), confirming that the transition in M4 was slower than in
477 M2, and the final ^{14}C ratio was also lower.
478
479 Both M2 and M4 started with archaeal communities dominated by the acetoclastic
480 *Methanosaetaceae*; but the final community compositions were different, with
481 *Methanobacteriaceae* being dominant in M2 and *Methanosarcinaceae* in M4. Yet it at first it
482 appeared as though the same route would be followed in both digesters as there was an initial
483 increase in hydrogenotrophic *Methanobacteriaceae* from day 55 to 77 in M4, similar to that in
484 M2 between days 104 to 126. In both M2 and M4 this was likely to have been in response to
485 the increase in TAN concentration, leading to inhibition of acetoclastic methanogenesis and a
486 temporary rise in acetic acid. In M2 at lower OLR the increase in acetic acid was less rapid,
487 and its decline probably occurred as a result both of the establishment of syntrophic acetate
488 oxidising bacteria (SAOB) and of a partial recovery in acetoclastic activity, as supported by
489 the observation of a temporary increase in *Methanosaetaceae* at the expense of
490 *Methanobacteriaceae* before the latter became fully established as the dominant methanogenic
491 family. A similar recovery in *Methanosaetaceae* was also observed in M4 between days 83 -
492 90, but the rise in acetic acid was more rapid and the total accumulation greater. The peak value
493 of 7 g L^{-1} acetic acid in M4 is outside the optimal range for *Methanosaetaceae*, which are
494 known to have a high acetate affinity linked to their ability to apply different systems for
495 activation, electron transfer and energy conservation (Smith and Ingram-Smith, 2007;
496 Westerholm et al., 2016). *Methanosarcinaceae* were favoured in M4, and their ability to utilise

497 a broad spectrum of substrates for methanogenesis including acetate, H_2 and CO_2, methanol
498 and methylamines (Thauer, Kaster et al., 2008; Liu, 2010) may have contributed towards this:
499 the fall in acetate concentration in M4 only occurred after a sharp increase in their relative
500 abundance. *Methanosarcinaceae* have recently been reported as being dominant in digestion
501 trials conducted at very high ammonia concentrations and relatively short HRT, using the
502 organic fraction of municipal solid waste (Yan et al., 2019) and cattle slurry with macroalgae
503 (Tian et al., 2018) as feedstocks: the results of the current work support this observed behaviour
504 and suggest HRT may have a role in promoting it. Neither of these previous studies carried out
505 ^{14}C determination, but Yan et al. (2019) suggested a potential shift by the dominant
506 *Methanosarcina soligelidi* to hydrogenotrophic metabolism while Tian et al. (2018) interpreted
507 an increase in the abundance of SAOB as indicating significant hydrogenotrophic activity.
508
509 It is clear that establishment of a SAOB population plays an essential role in the transition from
510 acetoclastic to hydrogenotrophic methanogenesis. Westerholm et al. (2016) noted, however,
511 that the doubling time for syntrophy between SAOB and hydrogenotrophic methanogens can
512 range from 9-78 days, and may also involve a lag phase before inception: one batch study
513 reported 49-54 days and 62-70 days for the initiation of syntrophy in thermophilic and
514 mesophilic digesters, respectively (Hao et al., 2017). The longer retention time in M2 could
515 thus have been a major contributor to the smooth transition in this digester, as the rate of
516 increase in TAN was lower and the onset of acetic acid accumulation occurred much later than
517 in M4. This would have allowed a longer period for the build-up of an SAOB population in
518 M2, responding to the competitive availability of acetic acid and facilitating a transition to
519 hydrogenotrophic methanogenesis mediated through the *Methanobacteriaceae*. M4 had a
520 shorter HRT, reached the inhibitory TAN threshold earlier than M2, and the higher organic
521 loading led to higher acetic acid production. Any or all of these factors may have caused or

522 contributed to a delay in the establishment of a SAOB population in M4; thus promoting
523 *Methanosarcinacea*, with its greater metabolic versatility, as the dominant methanogenic
524 community member in this case.
525
526 The slower increase in the ^{14}C ratio and the lower final value in M4 compared to M2 indicate
527 that a significant fraction of methanogenesis in M4 was still via the acetoclastic route, despite
528 the very marked shift in the dominant population. These results therefore strongly suggest that
529 the *Methanosarcinaceae* present are generating methane by both pathways simultaneously,
530 with different species in the community or perhaps even different individuals within one
531 species utilising different metabolic routes. A recent study based on metatranscriptomics has
532 shown *Methanosarcina thermophila* simultaneously performing acetoclastic,
533 hydrogenotrophic, and methylotrophic methanogenesis in acetate-fed thermophilic digesters
534 (Zhu et al., 2020): the current trial provides additional evidence for this simultaneous multi-
535 trophic metabolism and is the first time this has been reported in conventional mesophilic
536 digestion.
537
538 It should be noted that conditions during the ^{14}C labelling assay do not fully replicate those in
539 the digester, and this could potentially influence the outcome of the assay. For example, the
540 presence of anaerobic medium in the serum bottle provides dilution, which may reduce the
541 TAN concentration in an ammonia-rich digestate below the inhibitory threshold. In this case
542 some revival of acetoclastic methanogenesis could occur, particularly if members of the
543 community are already capable of utilising both metabolic routes. A major switch in metabolic
544 pathway or community structure appears unlikely within the relatively short 48-hour assay
545 period; but this aspect should be considered in future studies using this type of approach. In the
546 current study the TAN concentrations of M2 and M4 were similar from day 112 onwards, but

547 only M4 had a population dominated by the metabolically versatile *Methanosarcinaceae*. This
548 dominance was maintained consistently from day 97 onwards, representing 93% or more of
549 the archaeal population in the last four weeks of operation.
550
551 In the last part of the experimental period both M2 and M4 showed residual concentrations of
552 acetate in the range 0.5 - 1.5 g L^{-1} (as acetic acid), combined with high pH and TAN
553 concentrations. In these conditions the dominant species produced in acetogenesis is acetate
554 and the proportion present as molecular acetic acid, which is the form taken up by microbial
555 biomass, will be very low (Wilson et al., 2012). In M4 this residue may thus partly reflect the
556 relatively low affinity of *Methanosarcinceae* for acetate (Smith and Ingram-Smith, 2007; De
557 Vrieze et al., 2012). In both digesters, however, the dominant metabolic route in this period
558 was hydrogenotrophic. Under standard conditions, the oxidation of acetic acid to CO_2 and H_2
559 is a non-spontaneous reaction. For it to occur the ratio of the relative amounts of products to
560 reactants in the digester must be very low. This may have contributed to the presence of a
561 detectable acetic acid concentration, at least during this adaptation period. Despite differences
562 in their community structure and metabolic carbon flow, these conditions were achieved in
563 both M2 and M4, and both digesters showed a successful transition to accommodate the
564 selective pressure of an elevated TAN concentration.
565
566 In contrast, digesters M1 and M3 both failed to make such a transition and suffered VFA
567 accumulation and inhibition of methanogenesis. This was as expected, and confirms once again
568 the importance of trace elements in enabling syntrophic acetate oxidation coupled with
569 hydrogenotrophic methanogenesis. M1 and M3 were only sampled twice for 16S rRNA
570 amplicon sequencing, on days 70 and 126 for M1 and days 55 and 83 for M3. The number of
571 OTUs for these digesters was not significantly different from those for M2 and M4, with 195

572 and 185 OTUs in M1 and M3 respectively. The relative abundance of bacteria in each case was
573 also similar to that for the equivalent digester with TE addition on the same date
574 (Supplementary Information Figure S1). M1 showed the start of a similar transition in
575 community to that seen in M2, with the relative abundance of *Methanosaetaceae* falling from
576 94.1% to 54.5% and of *Methanobacteriaceae* rising from 4.6% to 36.4% from day 70 to day
577 126, although the proportion of other Euryarchaeota was slightly higher in M1 on day 126 at
578 6.1%. On day 55 relative abundance of *Methanosaetaceae* was slightly lower in M3 at 80.9%,
579 compared to 92.9% in M4, with the difference mainly represented by additional
580 *Methanobacteriaceae* in M3; but by day 83 the two digesters were similar with
581 *Methanosaetaceae* remaining dominant. The initiation of a change in the population structure
582 was therefore visible, especially in M1; but without TE supplementation this transition could
583 not be completed. This observation supports the view that a lack of vital metallo-enzymes
584 caused by trace element deficiencies is likely to be the primary reason for failure in these
585 conditions (Banks et al., 2012), rather than any differences in methanogenic population. There
586 was thus no opportunity for establishment of a stable alternative pathway mediated by more
587 ammonia-tolerant methanogens, and as expected both digesters without TE supplementation
588 failed as a result of inhibition of acetoclastic methanogenesis.
589
590 The unsupplemented digester M1 showed a small rise in acetic acid concentration to around 1
591 g L^{-1} between day 77 - 97 which was nearly identical to that also seen in M2 (Figure 1a). The
592 reason for this is unknown, but may have been related to the increasing pH in this period linked
593 with the rising TAN concentrations, and the consequent effects on acetic acid speciation and
594 availability. If it is assumed that the COD value of food waste is approximately 1.4 g COD g^{-1}
595 VS, however, and that 70% of this is converted to acetic acid in the acetogenesis stage, then
596 the residual concentration of 1 g L^{-1} represents only around 2% of the estimated daily

production; thus indicating that there was no major metabolic blockage whichever methanogenic route was being utilised at this point. Neither M3 nor M4 showed a distinct step of this type, although a slow rise in acetic acid concentrations was visible before the main peak.

3.3.5 Semi-quantification of metabolic functionality using ^{14}C equation

Figure 4a shows the estimated proportion of methane generated by the acetoclastic route in M1 - M4, based on Equation 1. The acetoclastic contribution in M1 and M3 without TE supplementation remained consistently high and close to the values seen in M2 and M4 (TE supplemented) on the same dates, until monitoring of M1 and M3 was stopped. In M2 and M4 the equation-derived values show a strong trend in the dominant pathway, as expected since these reflect the changes in the ^{14}C ratio in each case.

The ^{14}C ratio has previously been mainly regarded as a qualitative indicator, with values in excess of 1 taken as indicating a dominantly hydrogenotrophic pathway (Fotidis et al., 2013). The derivation of the relationship in Equation 1 is itself based on a number of assumptions and simplifications, including the importance of the affinity of the micro-organisms involved for lighter isotopes, and the proportion of dissolved CO_2 present (Jiang et al., 2018). The current study, however, is one of the first to look in detail at the period of transition from a predominately acetoclastic to a predominantly hydrogenotrophic community; the strong trends seen for digesters M2 and M4 in Figure 4 support the view that the ^{14}C ratio and the values obtained from the equation are at least semi-quantitative, and can be used to compare the proportion of each metabolic route being utilised in digesters operating under similar conditions.

During the trial it was noted that the proportion of labelled acetate remaining in the sample at the end of the ^{14}C assay was approximately constant in all four digesters from day 14-40, but rose in digesters M2 and M4 towards the end of the experiment (Figure 3b). This increase began earlier in M4 than M2 but the final value was higher in M2, mirroring the transition to hydrogenotrophic methanogenesis in each case. A possible explanation for these observations could be that the rate of conversion of acetic acid by the syntrophic acetate oxidation pathway is considerably lower than for acetoclastic methanogenesis (Schnürer et al., 1999); thus as the proportion of methane produced by the hydrogenotrophic route increases, the amount of labelled acetate converted in the fixed-duration assay decreases and the residue increases. If this explanation is correct, it provides another indicator of the transition in methanogenic pathway which is independent of the ^{14}C ratio. Figure 4c shows the residual labelled acetate as a proportion of the total amount added, plotted against the estimated proportion of methane produced by the acetoclastic route (calculated from Equation 1 and based on the ^{14}C ratio), for the whole experimental period for digesters M2 and M4 operating at OLR 3 and 5 g VS L day^{-1} respectively. Regression analysis showed reasonably strong relationships (M2 $R^2 = 0.7491$, n = 20; M4 $R^2 = 0.8179$, n = 19, with $p < 10^{-6}$ in each case), while t-testing confirmed that the slopes of -0.73 for M2 and -0.62 for M4 were not significantly different ($p > 0.3$), despite the different OLR and HRT in these two digesters. These results provide evidence of a clear relationship between two independent measures of the degree of transition between pathways, and further support the view that values obtained from Jiang's equation are at least semi-quantitative in nature and can be used to compare digesters operating under different conditions.

The ^{14}C ratio and the values obtained from Equation 1, in conjunction with the relative abundance of the dominant methanogenic families, provided a clear picture of the occurrence and duration of the critical transition period. In M2 this occurred over 28 days compared to 56

647 days in M4, equivalent to 0.4 and 1.3 HRT for the respective digesters. It is evident that the
648 transition is much more strongly influenced by the change in digester conditions than by
649 washout of microbial populations. The time required for transition is comparable with that for
650 the rise in VFA which indicated kinetic uncoupling of VFA and methane production in M1 and
651 M3. In both cases the change was quite rapid, especially in comparison with the very long slow
652 build-up of propionic acid previously observed in reactors operating on similar food waste
653 feedstocks at lower OLR (Banks et al., 2011, 2012).
654
655 Previous researchers have used batch studies to determine the metabolic pathways and
656 dominant species in anaerobic systems at very high ammonia concentrations. Fotidis et al.
657 (2013) and Tian et al. (2019) both found *Methanosarcinaceae* to be dominant or near-dominant
658 in acclimated batch cultures, with a strongly acetoclastic metabolic pathway (^{14}C ratio < 0.1 at
659 3 g N L^{-1} or above in mesophilic conditions, corresponding to 90% or more acetoclastic
660 methanogenesis according to Equation 1). These results at first sight may appear to conflict
661 with those of the current study. Fotidis et al. (2013) also tested non-acclimated inoculum,
662 however, and noted that in the mesophilic system an elevated ammonia concentration resulted
663 in a change from acetoclastic to hydrogenotrophic metabolism with a ^{14}C ratio of 4 or more,
664 which corresponds to over 80% hydrogenotrophic methanogenesis based on Equation 1. In the
665 current study comparative results from the ^{14}C assay were not available after day 155, but it is
666 intriguing to note that in the last two weeks of operation of M4 the ^{14}C ratio fell to below 1.8
667 (Figure 2), indicating an increase in acetoclastic methanogenesis with over one third of
668 methane production now coming from this route. During this period the abundance of
669 *Methanosarcinaceae* was unchanged, thus suggesting a further shift by this versatile family to
670 a preferred metabolic pathway. The current work makes it clear that OLR and HRT play an
671 important role in determining the transition to a dominant community and pathway in digesters

672 fed on real organic feedstocks; and thus may partially explain some of the otherwise apparently
673 conflicting results in the literature on batch and semi-continuous systems at high ammonia
674 concentrations (Fotidis et al., 2013; Hao et al., 2017; Yan et al., 2018).
675
676 Regression analysis was also conducted between the estimated percentage of methane
677 produced by the acetoclastic route and the relative abundance of dominant families during the
678 transition periods. The results for *Methanosaetaceae*, declining from dominance in the
679 respective transition periods, are shown in Figure 4d and indicate reasonably strong
680 relationships in both M2 (days 118-146; $n = 5$, $p < 0.05$) and M4 (days 97-146, $n = 8$, $p <$
681 0.005). Similar but inverse relationships between the percentage of methane produced by the
682 acetoclastic route and the relative abundance of the increasing hydrogenotrophic population
683 were also found in these periods for *Methanobacteriaceae* ($R^2 = 0.732$, $p = 0.06$) in M2 and
684 *Methanosarcinaceae* ($R^2 = 0.760$, $p < 0.005$) in M4. Despite the fact that the 16S rRNA
685 technique may include material from inactive microbes, the genetic analysis thus showed
686 relatively good agreement with the ^{14}C analysis, providing added confidence in the results from
687 both methods, the applicability of Equation 1, and the overall interpretation of the transition
688 period data. Observation of changes during a transition period can thus support and
689 complement previous studies reporting steady-state values from digesters in operation under
690 different conditions.
691
692 **4 Conclusions**
693
694 The pattern of change in the chemical characteristics of the digesters in response to increasing
695 ammonia concentrations was typical of that previously reported when using source segregated
696 food waste as feedstock. Addition of trace elements was essential to prevent rapid accumulation

of VFA at an otherwise inhibitory ammonia concentration, as demonstrated in previous studies. As expected, at the loadings used the initial peak in VFA was sufficient to cause a fall in pH and in specific methane production in unsupplemented digesters. The work confirmed that where trace elements were added, the digestion process was resilient to the rise in ammonia concentration and transitioned smoothly from a predominantly acetoclastic to a predominantly hydrogenotrophic metabolic route. This change could be monitored using the ^{14}C labelling technique, and under the lower loaded conditions at a higher HRT the gradual change in $^{14}CO_2$ /$^{14}CH_4$ ratio reflected the increasing predominance of hydrogenotrophic *Methanobacteriaceae* within the archaeal community. The slower rate of transition and the lower final $^{14}CO_2$ /$^{14}CH_4$ ratio seen at the higher loading and shorter HRT, coupled with the strong predominance of *Methanosarcinaceae* in the archaeal community, indicated that both acetoclastic and hydrogenotrophic pathways were being used by members of this group, which is known to have metabolic capability for both routes. This is the first time evidence of such simultaneous multi-trophic behaviour has been reported in conventional anaerobic digestion. It can be concluded that the make-up of the archaeal community and the dominant metabolic pathway is not solely due to relative tolerance to ammonia, and can be influenced by other factors including OLR or HRT or both. Monitoring of the transition also gave strong support to the idea that analysis of the $^{14}CO_2$ /$^{14}CH_4$ ratio can be used to provide an estimate of the proportion of methane produced by the acetoclastic and hydrogenotrophic routes which is at least semi-quantitative in nature, thus enabling comparisons between digesters working under different operating conditions. The results also provide an insight into how the archaeal population could be manipulated to increase hydrogenotrophic activity, which may have a useful purpose in future applications such as microbial CO_2 reduction.

Data accessibility

Raw, unprocessed fastq data were deposited to the European Nucleotide Archive and can be accessed from PRJEB30275 study.

Acknowledgements

This work was carried out with support from the Engineering and Physical Sciences Research Council through the IBCat H2AD project (EP/M028208/1). JPJC is a Royal Society Industry Fellow (IF160022)

References

Angelidaki, I. and Ahring, B.K., 1993. Thermophilic anaerobic digestion of livestock waste: the effect of ammonia. *Applied microbiology and biotechnology*, *38*(4), pp.560-564.

APHA, 2005. Standard methods for the examination of water and wastewater. *American Public Health Association (APHA): Washington, DC, USA*.

Aryal, N., Kvist, T., Ammam, F., Pant, D. and Ottosen, L.D., 2018. An overview of microbial biogas enrichment. *Bioresource technology*, *264*, pp.359-369.

Banks, C., Heaven, S., Zhang, Y. and Baier, U., 2018. Food waste digestion: anaerobic digestion of food waste for a circular economy. IEA Task 37 Technical Brochure. Available http://task37.ieabioenergy.com/technical-brochures.html, last accessed September 2019.

Banks, C.J., Chesshire, M. and Stringfellow, A., 2008. A pilot-scale comparison of mesophilic and thermophilic digestion of source segregated domestic food waste. *Water science and technology*, *58*(7), pp.1475-1481.

Banks, C.J., Chesshire, M., Heaven, S. and Arnold, R., 2011. Anaerobic digestion of source-segregated domestic food waste: performance assessment by mass and energy balance. *Bioresource technology*, *102*(2), pp.612-620.

746 Banks, C.J., Zhang, Y., Jiang, Y. and Heaven, S., 2012. Trace element requirements for stable
747 food waste digestion at elevated ammonia concentrations. *Bioresource technology*, *104*,
748 pp.127-135.
749 Callahan, B.J., McMurdie, P.J., Rosen, M.J., Han, A.W., Johnson, A.J.A. and Holmes, S.P.,
750 2016. DADA2: high-resolution sample inference from Illumina amplicon data. *Nature*
751 *methods*, *13*(7), p.581.
752 De Vrieze, J., Hennebel, T., Boon, N. and Verstraete, W., 2012. Methanosarcina: the
753 rediscovered methanogen for heavy duty biomethanation. *Bioresource technology*, *112*, pp.1-
754 9.
755 Environment Agency, 2007. The determination of chemical oxygen demand in waters and
756 effluents. In: Methods for the examination of waters and associated materials, Standing
757 Committee of Analysts. Available
758 https://assets.publishing.service.gov.uk/government/uploads/system/uploads/attachment_dat
759 a/file/755569/COD-215nov.pdf, last accessed June 2020.
760 Fotidis, I.A., Karakashev, D. and Angelidaki, I., 2014. The dominant acetate degradation
761 pathway/methanogenic composition in full-scale anaerobic digesters operating under
762 different ammonia levels. *International Journal of Environmental Science and Technology*,
763 *11*(7), pp.2087-2094.
764 Fotidis, I.A., Karakashev, D., Kotsopoulos, T.A., Martzopoulos, G.G. and Angelidaki, I., 2013.
765 Effect of ammonium and acetate on methanogenic pathway and methanogenic community
766 composition. *FEMS microbiology ecology*, *83*(1), pp.38-48.
767 Hao, L.P., Mazéas, L., Lü, F., Grossin-Debattista, J., He, P.J. and Bouchez, T., 2017. Effect of
768 ammonia on methane production pathways and reaction rates in acetate-fed biogas processes.
769 *Water Science and Technology*, *75*(8), pp.1839-1848.

770 Jerris, J.S. and McCarty, P.L., 1965. The Biochemistry of methane fermentation using C14
771 tracers. *J. Water Poll. Control Fed.*, *39*, pp.178-192.
772 Jiang, Y., Banks, C., Zhang, Y., Heaven, S. and Longhurst, P., 2018. Quantifying the
773 percentage of methane formation via acetoclastic and syntrophic acetate oxidation pathways
774 in anaerobic digesters. *Waste Management*, *71*, pp.749-756.
775 Jiang, Y., McAdam, E., Zhang, Y., Heaven, S., Banks, C. and Longhurst, P., 2019. Ammonia
776 inhibition and toxicity in anaerobic digestion: A critical review. *Journal of Water Process*
777 *Engineering*, *32*, p.100899.
778 Jones, J.B. and Stadtman, T.C., 1981. Selenium-dependent and selenium-independent formate
779 dehydrogenases of Methanococcus vannielii. Separation of the two forms and
780 characterization of the purified selenium-independent form. *Journal of Biological Chemistry*,
781 *256*(2), pp.656-663.
782 Karakashev, D., Batstone, D.J. and Angelidaki, I., 2005. Influence of environmental conditions
783 on methanogenic compositions in anaerobic biogas reactors. *Appl. Environ. Microbiol.*, *71*(1),
784 pp.331-338.
785 Karakashev, D., Batstone, D.J., Trably, E. and Angelidaki, I., 2006. Acetate oxidation is the
786 dominant methanogenic pathway from acetate in the absence of Methanosaetaceae. *Appl.*
787 *Environ. Microbiol.*, *72*(7), pp.5138-5141.
788 Koster, I.W. and Lettinga, G., 1984. The influence of ammonium-nitrogen on the specific
789 activity of pelletized methanogenic sludge. *Agricultural wastes*, *9*(3), pp.205-216.
790 Liu, Y. (2010). Methanosarcinales. Handbook of Hydrocarbon and Lipid Microbiology. K. N.
791 Timmis. Berlin, Heidelberg, Springer Berlin Heidelberg: 595-604.
792 Lü, F., Zhou, Q., Wu, D., Wang, T., Shao, L. and He, P., 2015. Dewaterability of anaerobic
793 digestate from food waste: relationship with extracellular polymeric substances. *Chemical*
794 *Engineering Journal*, *262*, pp.932-938.

795 Luo, G. and Angelidaki, I., 2013a. Co-digestion of manure and whey for in situ biogas
796 upgrading by the addition of H 2: process performance and microbial insights. *Applied*
797 *microbiology and biotechnology*, *97*(3), pp.1373-1381.
798 Luo, G., Wang, W. and Angelidaki, I., 2013b. Anaerobic digestion for simultaneous sewage
799 sludge treatment and CO biomethanation: process performance and microbial ecology.
800 *Environmental science & technology*, *47*(18), pp.10685-10693.
801 McCarty, P.L., 1964. Anaerobic waste treatment fundamentals. *Public works*, *95*(9), pp.107-
802 112.
803 Molaey, R., Bayrakdar, A., Sürmeli, R.Ö. and Çalli, B., 2018. Anaerobic digestion of chicken
804 manure: Mitigating process inhibition at high ammonia concentrations by selenium
805 supplementation. *Biomass and Bioenergy*, *108*, pp.439-446.
806 Quast, C., Pruesse, E., Yilmaz, P., Gerken, J., Schweer, T., Yarza, P., Peplies, J. and Glöckner,
807 F.O., 2012. The SILVA ribosomal RNA gene database project: improved data processing and
808 web-based tools. *Nucleic acids research*, *41*(D1), pp.D590-D596.
809 Rajagopal, R., Massé, D.I. and Singh, G., 2013. A critical review on inhibition of anaerobic
810 digestion process by excess ammonia. *Bioresource technology*, *143*, pp.632-641.
811 Resch, C., Wörl, A., Waltenberger, R., Braun, R. and Kirchmayr, R., 2011. Enhancement
812 options for the utilisation of nitrogen rich animal by-products in anaerobic digestion.
813 *Bioresource technology*, *102*(3), pp.2503-2510.
814 Schnürer, A. and Nordberg, Å., 2008. Ammonia, a selective agent for methane production by
815 syntrophic acetate oxidation at mesophilic temperature. *Water Science and Technology*, *57*(5),
816 pp.735-740.
817 Schnürer, A., Zellner, G. and Svensson, B.H., 1999. Mesophilic syntrophic acetate oxidation
818 during methane formation in biogas reactors. *FEMS microbiology ecology*, *29*(3), pp.249-
819 261.

820 Serna-Maza, A., Heaven, S. and Banks, C.J., 2014. Ammonia removal in food waste anaerobic
821 digestion using a side-stream stripping process. *Bioresource technology*, *152*, pp.307-315.
822 Smith, K.S. and Ingram-Smith, C., 2007. Methanosaeta, the forgotten methanogen?. *Trends in*
823 *microbiology*, *15*(4), pp.150-155.
824 Sun, C., Cao, W., Banks, C.J., Heaven, S. and Liu, R., 2016. Biogas production from undiluted
825 chicken manure and maize silage: a study of ammonia inhibition in high solids anaerobic
826 digestion. *Bioresource Technology*, *218*, pp.1215-1223.
827 Tao, B., Alessi, A.M., Zhang, Y., Chong, J.P., Heaven, S. and Banks, C.J., 2019. Simultaneous
828 biomethanisation of endogenous and imported CO2 in organically loaded anaerobic digesters.
829 *Applied energy*, *247*, pp.670-681.
830 Thauer, R.K., Kaster, A.K., Seedorf, H., Buckel, W. and Hedderich, R., 2008. Methanogenic
831 archaea: ecologically relevant differences in energy conservation. *Nature Reviews*
832 *Microbiology*, *6*(8), pp.579-591.
833 Tian, H., Fotidis, I.A., Mancini, E., Treu, L., Mahdy, A., Ballesteros, M., González-Fernández,
834 C. and Angelidaki, I., 2018. Acclimation to extremely high ammonia levels in continuous
835 biomethanation process and the associated microbial community dynamics. *Bioresource*
836 *technology*, *247*, pp.616-623.
837 Van Velsen, A.F.M., 1979. Adaptation of methanogenic sludge to high ammonia-nitrogen
838 concentrations. *Water Research*, *13*(10), pp.995-999.
839 Walker, M., Zhang, Y., Heaven, S. and Banks, C., 2009. Potential errors in the quantitative
840 evaluation of biogas production in anaerobic digestion processes. *Bioresource technology*,
841 *100*(24), pp.6339-6346.
842 Westerholm, M., Moestedt, J. and Schnürer, A., 2016. Biogas production through syntrophic
843 acetate oxidation and deliberate operating strategies for improved digester performance.
844 *Applied energy*, *179*, pp.124-135.

845 Wilson, C.A., Novak, J., Takacs, I., Wett, B. and Murthy, S., 2012. The kinetics of process
846 dependent ammonia inhibition of methanogenesis from acetic acid. *Water research*, *46*(19),
847 pp.6247-6256.
848 Wood, G.E., Haydock, A.K. and Leigh, J.A., 2003. Function and regulation of the formate
849 dehydrogenase genes of the methanogenic archaeon Methanococcus maripaludis. *Journal of*
850 *bacteriology*, *185*(8), pp.2548-2554.
851 Yan, M., Fotidis, I.A., Tian, H., Khoshnevisan, B., Treu, L., Tsapekos, P. and Angelidaki, I.,
852 2019. Acclimatization contributes to stable anaerobic digestion of organic fraction of
853 municipal solid waste under extreme ammonia levels: focusing on microbial community
854 dynamics. *Bioresource technology*, *286*, p.121376.
855 Yenigün, O. and Demirel, B., 2013. Ammonia inhibition in anaerobic digestion: a review.
856 *Process Biochemistry*, *48*(5-6), pp.901-911.
857 Yirong, C., Heaven, S. and Banks, C.J., 2015. Effect of a trace element addition strategy on
858 volatile fatty acid accumulation in thermophilic anaerobic digestion of food waste. *Waste and*
859 *Biomass Valorization*, *6*(1), pp.1-12.
860 Yirong, C., Heaven, S. and Banks, C.J., 2015. Effect of a trace element addition strategy on
861 volatile fatty acid accumulation in thermophilic anaerobic digestion of food waste. *Waste and*
862 *Biomass Valorization*, *6*(1), pp.1-12.
863 Yirong, C., Zhang, W., Heaven, S. and Banks, C.J., 2017. Influence of ammonia in the
864 anaerobic digestion of food waste. *Journal of environmental chemical engineering*, *5*(5),
865 pp.5131-5142.
866 Zhang, W., Heaven, S. and Banks, C.J., 2017a. Continuous operation of thermophilic food
867 waste digestion with side-stream ammonia stripping. *Bioresource technology*, *244*, pp.611-
868 620.

869 Zhang, W., Heaven, S. and Banks, C.J., 2017b. Thermophilic digestion of food waste by
870 dilution: ammonia limit values and energy considerations. *Energy & Fuels*, *31*(10), pp.10890-
871 10900.
872 Zhang, Y., Banks, C.J. and Heaven, S., 2012. Anaerobic digestion of two biodegradable
873 municipal waste streams. *Journal of Environmental Management*, *104*, pp.166-174.
874 Zhu, X., Campanaro, S., Treu, L., Seshadri, R., Ivanova, N., Kougias, P.G., Kyrpides, N. and
875 Angelidaki, I., 2020. Metabolic dependencies govern microbial syntrophies during
876 methanogenesis in an anaerobic digestion ecosystem. *Microbiome*, *8*(1), pp.1-14.
877
878 **Figures and Tables**
879

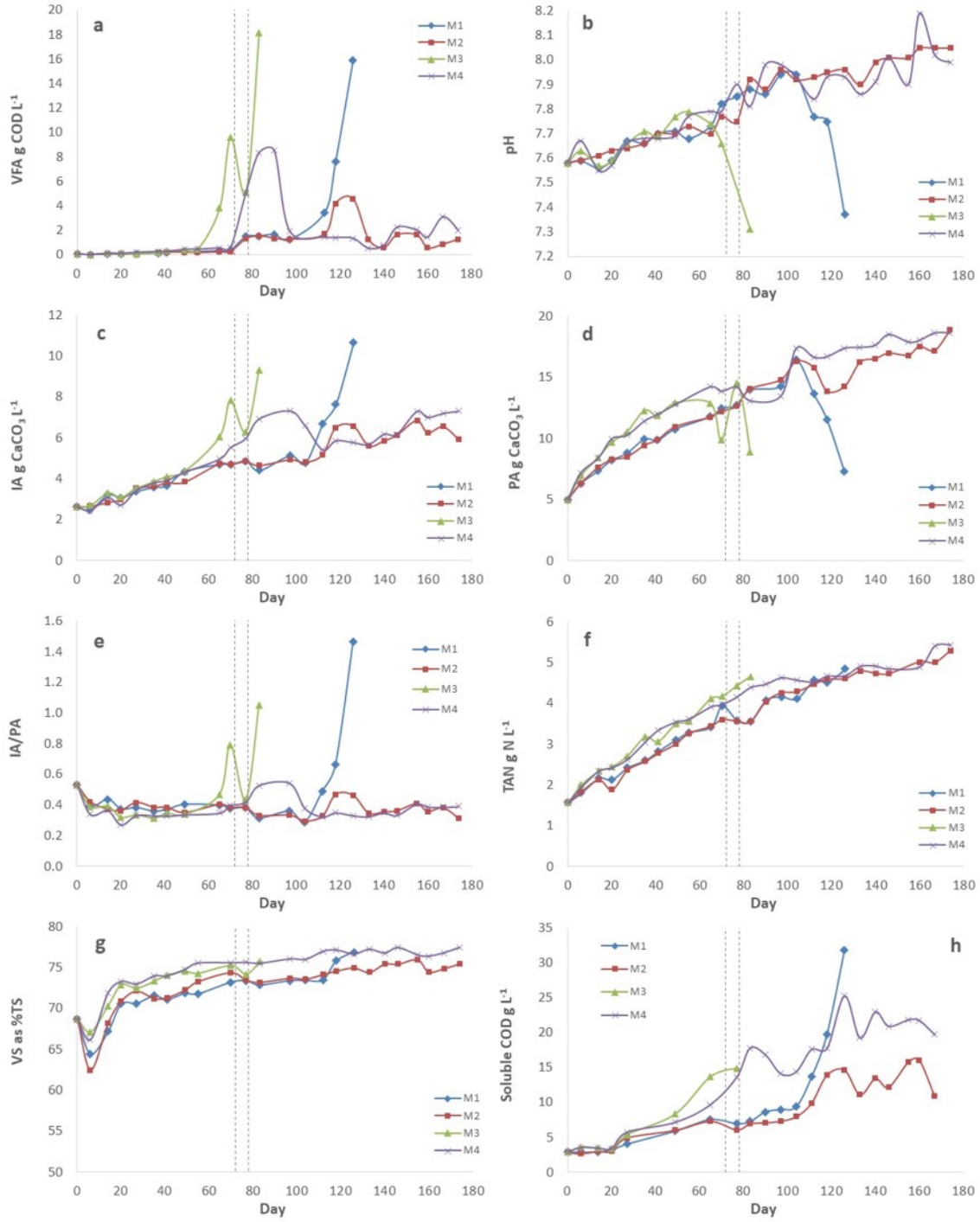

Figure 1 Selected monitoring parameters for all digesters during experimental period: (a) VFA, (b) pH, (c) IA, (d) PA, (e) IA/PA, (f) TAN, (g) VS/TS and (h) soluble COD. Vertical dotted lines indicate period when M3 was not fed.

880

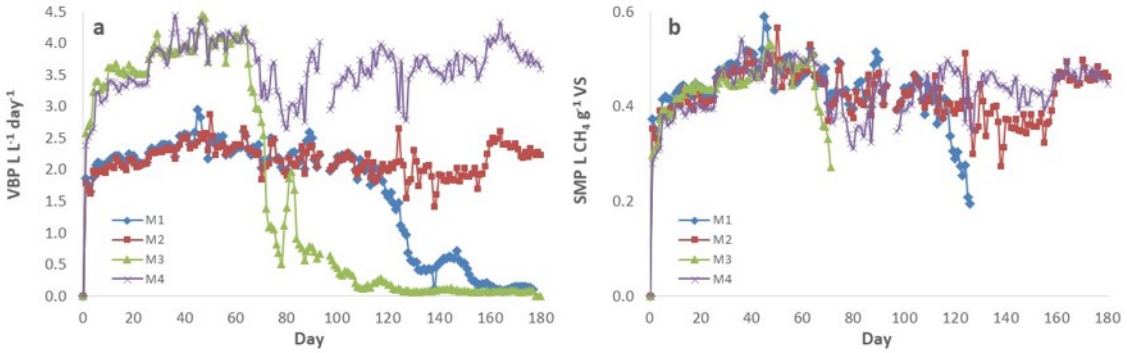

Figure 2 Gas production for all digesters during experimental period: (a) VBP, (b) SMP.

881

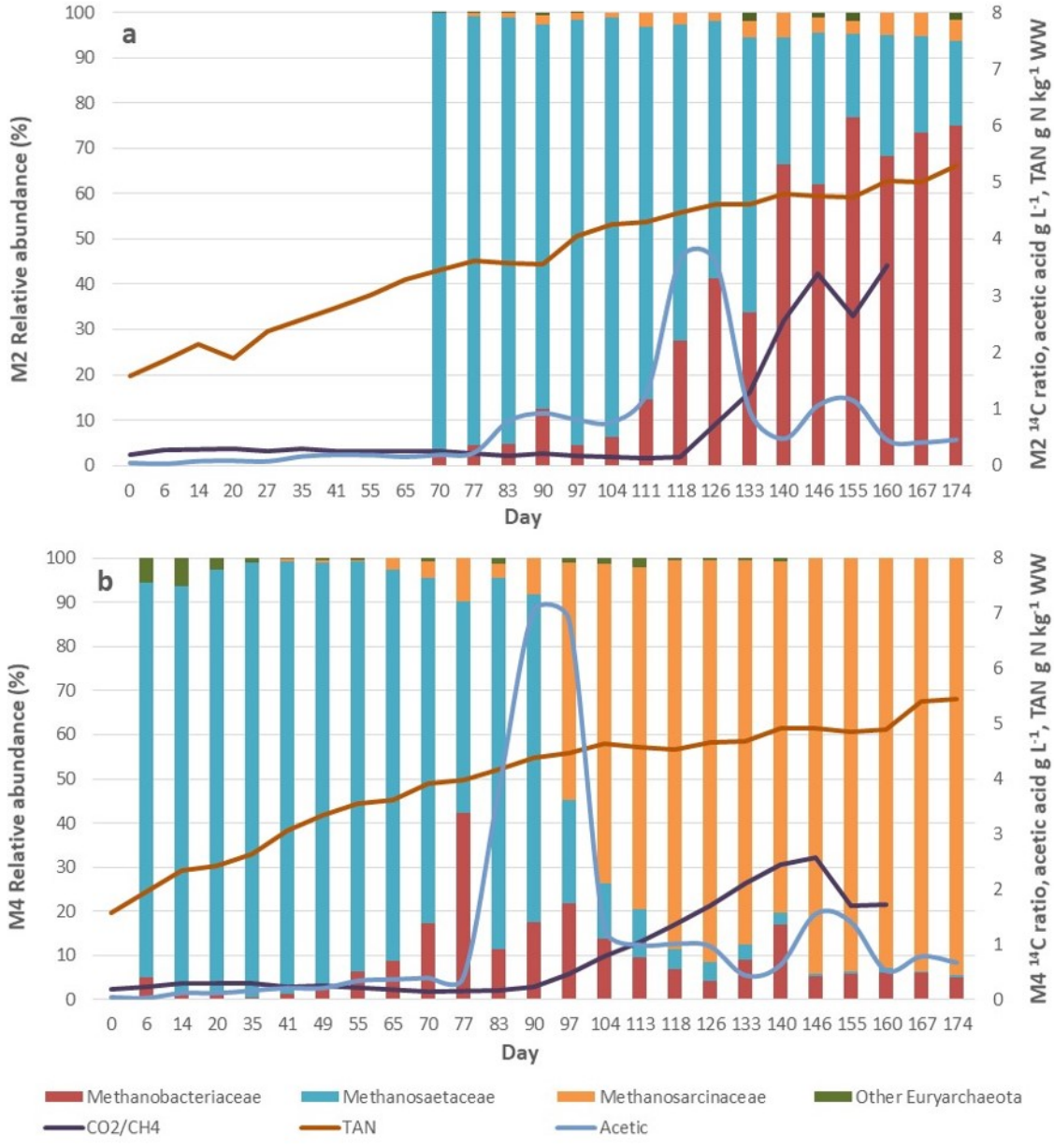

Figure 3 Relative abundance of archaeal groups, ^{14}C ratio, TAN and acetic acid concentrations in digesters: (a) M2 and (b) M4 during the experimental period

882

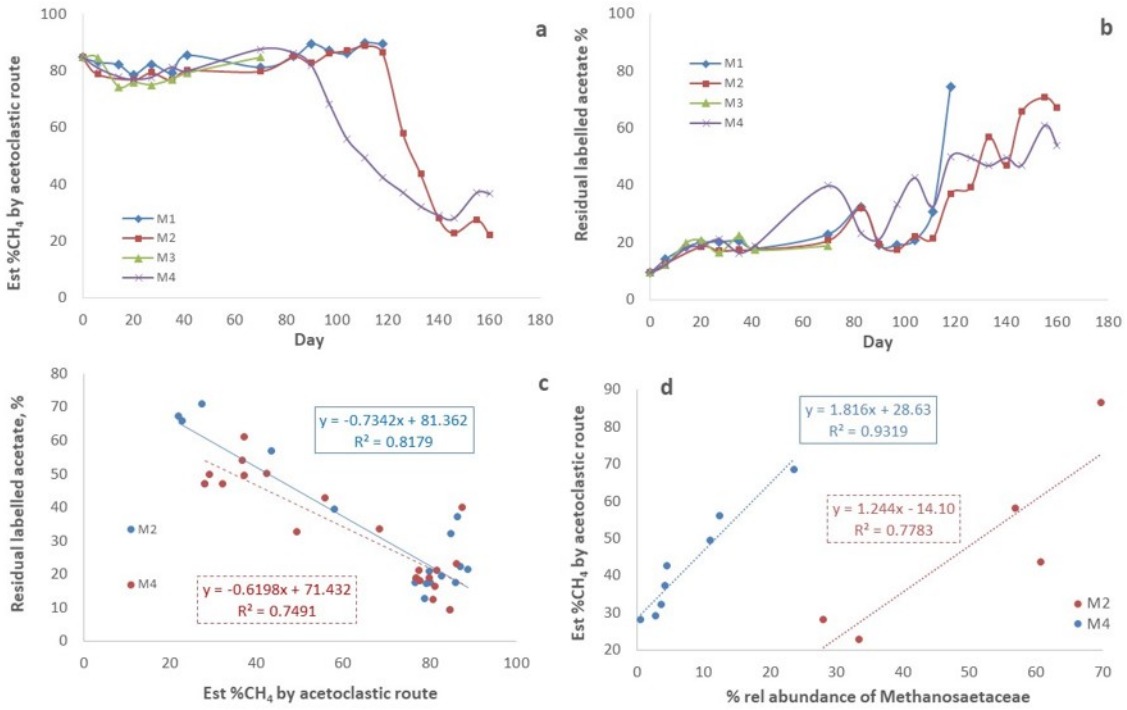

Figure 4 Results based on for ^{14}C assay and Equation 1: (a) Estimated proportion of CH_4 produced by acetoclastic route for digesters M1-4 against time; (b) residual labelled acetate in ^{14}C assay for digesters M1-4 against time; (c) Estimated proportion of CH_4 produced by acetoclastic route versus residual labelled acetate in ^{14}C assay for digesters M2 and M4; (d) Estimated proportion of CH_4 produced by acetoclastic route versus relative abundance of *Methanosaetaceae* during transition periods in digesters M2 and M4

883

884 **Table 1 Physicochemical characteristics of foodwaste**

Parameter	Units	Value		SD
Total solids	g TS kg^{-1} WW	238.5	±	1.2 [a]
Volatile solids	g VS kg^{-1} WW	206.8	±	2.1 [a]
TKN	g N kg^{-1} WW	7.0	±	0.12

Elemental C	% of TS	50.28	±	0.75
Elemental H	% of TS	6.37	±	0.07
Elemental N	% of TS	3.68	±	0.09
Carbohydrate	g kg^{-1} VS	492.1	±	12.5
Lipid	g kg^{-1} VS	197.0	±	2.2
Crude protein	g kg^{-1} VS	211.2	±	3.7
Calorific value	MJ kg^{-1} TS	22.0	±	0.06
	MJ kg^{-1} VS	25.4	±	0.06

885 SD = standard deviation for triplicate samples unless noted.

886 [a] 8 samples

887